

# Influence of compost amendments on the hydraulic functioning of brownfield soils

*"This is the peer reviewed version of the following article: A. Whelan, C. Kechavarzi, F. Coulon, R. Sakrabani, R. Lord, Influence of compost amendments on the hydraulic functioning of brownfield soils, Soil Use and Management, Volume 29, Issue 2, pages 260–270, June 2013, which has been published in final form at DOI: 10.1111/sum.12028. This article may be used for non-commercial purposes in accordance with [Wiley Terms and Conditions for Self-Archiving](#)."*

A. WHELAN<sup>1</sup>, C. KECHAVARZI<sup>1</sup>, F. COULON<sup>1</sup>, R. SAKRABANI<sup>1</sup> & R. LORD<sup>2</sup>

<sup>1</sup> *Department of Environmental Science and Technology, School of Applied Sciences, Cranfield University, MK43 0AL, Cranfield, UK, and* <sup>2</sup> *Department of Civil and Environmental Engineering, Faculty of Engineering, University of Strathclyde, G4 0NG, Glasgow, UK*

Correspondance: C. Kechavarzi. E-mail: [Cedric.Kechavarzi@gmail.com](mailto:Cedric.Kechavarzi@gmail.com)

**Running title:** Hydraulic properties of compost amended soils

## **Abstract**

This study assessed the impact of compost on the hydraulic properties of three soils (sandy loam, clay loam and diesel contaminated sandy loam) with relatively poor physical quality typical of brownfield sites. Soils were amended with two composts at 750 t/ha. Samples were also collected from a clay capped brownfield site, previously amended with 250, 500 or 750t/ha of compost. Water release characteristics and saturated hydraulic conductivity were determined for all soils and physical quality indicators derived. Unsaturated flow in field profiles after compost application with two depths of incorporation and two indigenous subsoils was simulated using Hydrus-1D. Compost generally increased water retention. Hydraulic conductivity tended to decrease following compost application in sandy loam but increased in clay and clay loam, where compost addition resulted in a larger dominant pore size. Although compost improved physical quality indicators, they remained sub-optimum in clay and clay loam soil, which exhibited poor aeration, and in the contaminated sandy loam, where available water capacity was limited, possibly due to changes in wettability. Increasing application rates in the field enhanced water retention at low potentials and hydraulic conductivity near saturation but did not alter physical quality indicators. Numerical simulation indicated that the 500 t/ha application resulted in the best soil moisture regime. Increasing the depth of incorporation in the clay cap improved drainage and reduced waterlogging but incorporation in more permeable subsoil resulted in prolonged dry conditions to greater depths.

**Keywords:** Compost, water release characteristics, hydraulic function, brownfield, land reclamation

## **Introduction**

Large stockpiles of compost are being produced due to European Union regulations to reduce the amount of degradable waste sent to landfill (Antizar-Ladislao et al, 2005). Consequently, opportunities to utilise compost to return brownfield land to productive use have received increasing attention. Compost can facilitate remediation (Semple et al, 2001), whilst improving the physical (Wanas and Omran, 2006), chemical (Said-Pullicino et al, 2010) and biological properties of degraded soils (Gandolfi et al, 2010). With increasing pressure on conventional land and since renewable energy targets advocate an expansion in energy crop production (Charles et al, 2007), one potential use for neglected land is biomass crop cultivation. Throughout the UK there have been several trials to establish biomass crops on degraded land (Riddell-Black, 2002), some of them using composts (Lord and Green, 2011) and often focussing on crop response to heavy metal contamination.

Soil productivity and contaminant fate and transport are related to the ability of the soil to infiltrate, transmit and store water. To sustain yields of bioenergy crops on degraded soils, whilst managing contamination risk, an understanding of the influence of organic amendments, like compost on soil physical and hydraulic properties is needed. Compost affects soil bulk density, water retention and hydraulic conductivity (Aggelides and Londra, 2000) through the modification of porosity. Consequently, infiltration, storage and drainage of water, gas exchange, solute and contaminant movement and ease of root penetration will also be affected (Reynolds et al, 2009). Organic contaminants, such as petroleum hydrocarbons also alter soil hydraulic characteristics through changes in interfacial and surface properties (Kechavarzi et al., 2005) resulting in reduced water retention and transmission (Hyun et al., 2008). Hence, although compost may have beneficial impacts on soil physical properties, the degree to which these improvements affect soil hydraulic properties requires further consideration. Finally, compost incorporation at the soil surface

will result in layered soil profiles whose hydraulic functioning is dependent on both the properties of the compost amended layer and the native soil but also incorporation depth and boundary conditions. Therefore, to develop appropriate compost application strategies, an understanding of the hydraulic functioning of the entire soil profile is needed.

The aim of this study was to assess, experimentally, the impact of compost on the hydraulic properties and physical quality of degraded soils. Additionally, numerical simulations were used to characterise the influence of these properties on the hydraulic functioning of a compost amended brownfield soil profile.

## **Materials and methods**

### *Laboratory and field samples*

The soils used to prepare homogenised laboratory samples consisted of a sandy loam and a clay loam sampled from Cranfield University farm. The soils were dried and sieved to 2mm. Part of the sandy loam was spiked with 12.5 g/kg diesel fuel and aged for approximately 30 months. The soils were mixed with two composts; one composed primarily of green waste (31% OM) and one composed of approximately half green waste and half catering meat waste (52% OM), hereafter referred to as green and meat composts respectively, at a rate equivalent to a field application of 750 t/ha assuming a 30 cm incorporation depth (45 and 62% compost by weight for the green and meat composts, respectively). The treatments were packed into cores, 6 cm in diameter and 5.4 cm deep ( $152 \text{ cm}^3$ ) and replicated 3 times to a similar mass and bulk density, ranging from  $0.4 \text{ g/cm}^3$  ( $\pm 0.02 \text{ g/cm}^3$ ) in the pure meat compost to  $1.23 \text{ g/cm}^3$  in the clay loam ( $\pm 0.02 \text{ g/cm}^3$ ) with a maximum variation of 7% between replicates. The compost densities ( $0.4$  and  $0.6 \text{ g/cm}^3$  for the green and meat composts, respectively) were similar to those of organic soils containing a large proportion of organic matter (Kechavarzi et al., 2010).

Field cores were also sampled from a compost-amended brownfield site. The site was a former sewage treatment works capped with clay to a depth of 0.8 m in Tyne and Wear, North East England. The site was amended with PAS100 compost in 2007 at three rates (250, 500 and 750 t/ha) and planted with four energy crops to assess the feasibility of using brownfield land for energy crop production (Lord et al., 2011). Three undisturbed cores were sampled at the surface (0-15 cm depth) for each application rate and at 15-30 cm depth in the underlying clay cap. Small metal cores (5 cm deep and 5.3 cm in diameter) were then used to sub-sample the top of the field cores for analysis.

Soil profile descriptions, to a depth of 0.5m on a 1m transect, were carried out under the three compost application rates. As the site was not representative of a conventional agricultural field, traditional soil profile descriptions were not possible and so focused on the depth of the compost layers, the presence of roots, stones and other materials and other distinctive features.

#### *Hydraulic functions and soil physical quality parameters*

Water release characteristics were measured using sand table apparatus at water potentials, expressed in water height equivalents, of 0, 30, 50 and 100 cm and pressure cell apparatus at pressure heads of 200, 500, 1000, 1500, 2000, 5000, 10000 and 15000 cm. The Van Genuchten (1980) equation was fitted to the water release curve data using the RETC code (Van Genuchten et al, 1991):

$$\theta = (\theta_{sat} - \theta_{res}) \left[ 1 + \left( \frac{1}{\alpha h} \right)^n \right]^{-m} + \theta_{res} \quad (1)$$

Where  $\theta$  is the moisture content,  $h$  is the pressure head,  $\theta_{sat}$  is the saturated moisture content,  $\theta_{res}$  (residual moisture content)  $\alpha$  and  $n$  are fitting parameters and  $m = 1 - 1/n$ .

The parameters of the water release curve were also used to obtain the predictive unsaturated hydraulic conductivity function derived by Van Genuchten (1980):

$$K(h) = K_{sat} \frac{\{1 - (\alpha h)^{mn} [1 + (\alpha h)^n]^{-m}\}^2}{[1 + (\alpha h)^n]^{ml}} \quad (2)$$

117 In which  $K(h)$  is the unsaturated hydraulic conductivity and  $K_{sat}$  is the saturated hydraulic  
 118 conductivity measured using a falling head permeameter.

119 Following Dexter (2004), Equation 1 was differentiated with respect to the natural  
 120 logarithm of the pressure head to give an indication of the pore size distribution, maximum  
 121 pore size and frequency of pores in this maximum pore class:

$$\frac{\partial \theta}{\partial \ln(h)} = -mn(\theta_{sat} - \theta_{res}) \alpha^n h^n [1 + (\alpha h)^n]^{-m-1} \quad (3)$$

122 The peak of the differentiated function (the inflection point of the release curve),  
 123 indicates where drainage is maximum and is characterised by its location and slope. The  
 124 location is given by the pressure  $h_i$  and occurs at (Dexter, 2004):

$$h_i = \frac{1}{\alpha} \left[ \frac{1}{m} \right]^{\frac{1}{n}} \quad (4)$$

125 with a corresponding water content,  $\theta_i$ :

$$\theta_i = (\theta_{sat} - \theta_{res}) \left[ 1 + \frac{1}{m} \right]^{-m} + \theta_{res} \quad (5)$$

126 The slope of the curve,  $S$ , at this point is the modulus of (Dexter, 2004):

$$S = \left| n(\theta_{sat} - \theta_{res}) \left[ 1 + \frac{1}{m} \right]^{-(1+m)} \right| \quad (6)$$

127 The water potential  $h_i$ , is representative of the dominant pore size of the soil where the  
 128 specific water capacity is greatest. Hence,  $S$  at this point can be considered as an overall  
 129 index of physical and structural quality and it has been correlated to other key soil quality  
 130 indicators such as bulk density and organic matter content (Dexter, 2004; Dexter and Czyz,  
 131 2007). Dexter (2004) classed soils with an  $S$  value of  $\geq 0.035$  (when  $\theta$ ,  $\text{g.g}^{-1}$ , is expressed on a  
 132 gravimetric basis) as being of good physical quality, while most soils studied by Dexter and  
 133 Czyz (2007) had an  $S$  value between 0.015 and 0.060.

134 For non-agricultural soils, Reynolds et al. (2009) suggest that S should be used in  
135 combination with other physical quality parameters especially for structureless or single grain  
136 materials such as composts. Hence, a series of other physical quality parameters (Reynolds et  
137 al., 2009) were measured to augment this index: the plant available water capacity (PAWC),  
138 defined as the difference between the moisture contents at 50 cm and at  $1.5 \times 10^4$  cm; the  
139 drainable porosity (DP) which is the proportion of air filled pores at field capacity calculated  
140 as the difference between the moisture contents at saturation and at 50 cm; and the relative  
141 field capacity (RFC) which indicates the ability of the soil to store water and air relative to  
142 the soils total pore volume and is calculated as the ratio of moisture content at 50 cm to that  
143 at saturation (Reynolds et al., 2009).

144

#### 145 *Numerical simulations*

146 The water regime of the field profiles, amended with compost at the rates of 250, 500 and  
147 750 t/ha, was simulated using the numerical model Hydrus-1D which uses linear finite  
148 element schemes to solve Richards' equation for saturated-unsaturated water flow (Simunek,  
149 2008). The size of the simulated 1D profile was 0.8m depth and consisted of two materials  
150 with a profile discretisation of 500 nodes. The top 0.1 m consisted of the compost-amended  
151 materials (soil profile descriptions showed this to be the incorporation depth across all rates  
152 in the field) and 0.7 m consisted of the underlying clay cap material. For each layer, the  
153 hydraulic parameters (Equations 1 and 2) used in the model were those obtained from the  
154 water release and hydraulic conductivity measurements carried out on the undisturbed field  
155 cores. In addition to the existing field profiles, alternative scenarios were considered to assess  
156 the impact of incorporation depth and indigenous soil type on the hydraulic functioning of  
157 such profiles. In the case where sandy loam was used as the indigenous subsoil, the hydraulic  
158 parameters used were those of the homogenised samples. In all simulations the upper

159 boundary was set as an atmospheric boundary with a maximum surface ponding of 0 mm  
160 allowed before the onset of run-off. This time variable boundary condition consisted of  
161 precipitation and daily potential evapotranspiration calculated using the Penman-Monteith  
162 equation (Allen, 1998) with meteorological data from a land surface station approximately 6  
163 miles from the field site (BADC, 2010). The simulation time was 2 years (2008 and 2009).  
164 The lower boundary was set to free drainage (zero-gradient boundary condition). An initial  
165 pressure head of 200 cm was applied to the entire profile. These simulations were primarily  
166 used for a qualitative appraisal of the influence of application rate, incorporation depth and  
167 indigenous soil type acknowledging that field variability could impact on water regime and  
168 that, in the case of the sandy loam subsoil, the homogenised samples used may not be  
169 representative of field conditions where structure may develop.

170

#### 171 *Statistical analysis*

172 ANOVA were carried out using Statistica 9 (Statsoft inc, 2010) for analysis of measured  
173 points of the water release curve, saturated and unsaturated hydraulic conductivity (using  
174 modelled values), Van Genuchten parameters and physical quality data. To ensure a balanced  
175 factorial design, one analysis excluded the two composts to evaluate the impact of compost  
176 on the different soils and one excluded the three unamended soils to analyse the impact of  
177 compost type. P values  $>0.05$  were considered not significant.

178

## 179 **Results and discussion**

### 180 *Hydraulic functions*

181 Water release characteristics were affected by the addition of compost but also by diesel  
182 contamination (Table 1, Figure 1). The diesel-spiked sandy loam (Figure 1c) had smaller  
183 water retention at all tensions ( $p<0.01$ ) and lower air entry pressure (larger  $\alpha$ ,  $p<0.02$ )



184 compared to the uncontaminated sandy loam, (Figure 1a). Saturated hydraulic conductivity  
185 was greater in the diesel-spiked soil ( $p < 0.01$ ) but unsaturated hydraulic conductivity was  
186 significantly less ( $p < 0.04$ ) for pressure heads ranging from 0 to  $2 \times 10^3$  cm (data not shown).  
187 These results agree with those of Hyun et al. (2008), who found reduced unsaturated  
188 hydraulic conductivity, less water retention and larger  $\alpha$  in a diesel contaminated soil  
189 compared to a bioremediated counterpart. The initial diesel concentration (12.5 g/kg in 2006)  
190 corresponded to a low residual volumetric diesel content of 1.7%, assuming a diesel density  
191 of  $0.8 \text{ g/cm}^3$ . Furthermore, the total petroleum hydrocarbon concentration measured in 2010  
192 had reduced to 83 mg/kg due to aging. This corresponded to a negligible volumetric content  
193 of 0.01% indicating no significant quantity of free phase diesel and unlikely changes in water  
194 content due to interfacial tension effects between free oil and aqueous phases. It is therefore  
195 plausible that the reduction in water retention and unsaturated hydraulic conductivity was due  
196 to the adsorption of organic compounds onto the soil, leading to a reduction in wettability, as  
197 well as their dissolution in water, which resulted in reduced interfacial tension between water  
198 and air. These potential changes in wettability were corroborated by Whelan et al. (2010)  
199 who measured apparent contact angles as high as  $141^\circ (\pm 10^\circ)$  on the same soil under dry  
200 conditions using the sessile drop method (Bachmann et al., 2000). It is also possible that the  
201 dominant pore size of the sandy loam (Figure 2a) increased following diesel addition (Figure  
202 2c), explaining the increase in saturated conductivity. Although not quantified, some  
203 aggregation was observed in the diesel-contaminated samples. This could explain the increase  
204 in macroporosity and is consistent with the findings of Martinho et al. (2009) who measured a  
205 20% increase in the proportion of aggregates between 0.05 and 0.5 mm 12 months after the  
206 addition of diesel to a loamy soil. They attributed this aggregation to diesel degrading  
207 microorganism activity.

208           The application of compost to the diesel-spiked soil (Figures 1c) resulted in increased  
209 water retention (significant for green compost at  $5 \times 10^3$ ,  $1 \times 10^4$  and  $1.5 \times 10^4$  cm pressures,  
210  $p < 0.04$ , and for meat compost at all pressures below 200 cm,  $p < 0.01$ ).  $\alpha$  and  $n$  remained  
211 unaltered but  $\theta_{res}$  increased significantly (Table 2,  $p < 0.05$ ). Saturated hydraulic conductivity  
212 decreased following the addition of both composts ( $p < 0.05$ ) but unsaturated hydraulic  
213 conductivity only decreased significantly between 30 and  $2 \times 10^3$  cm by the addition of meat  
214 compost ( $p < 0.04$ ). The large value of saturated hydraulic conductivity for diesel-spiked soil,  
215 which may be explained by aggregation, was reduced by the addition of compost, in contrast  
216 to results from other studies, and suggests that compost mostly resulted in an increase in  
217 hydraulic conductivity (Aggelides and Londra, 2000).

218           In contrast, green compost had no impact on water retention and unsaturated  
219 hydraulic conductivity of the uncontaminated sandy loam (Figure 1a). Meat compost,  
220 however, increased retention at pressures larger than  $10^3$  cm ( $p < 0.04$ ) and decreased  
221 unsaturated hydraulic conductivity at pressures less than  $5 \times 10^3$  cm ( $p < 0.04$ ). Saturated  
222 hydraulic conductivity was increased by green compost ( $p < 0.01$ ) but decreased with meat  
223 compost (Table 2). This increase in retention at higher pressures and decrease in conductivity  
224 following meat compost addition, combined with no significant increase in total porosity,  
225 suggests an increase in microporosity. The water release characteristics of the two composts  
226 (curves not shown) were not significantly different but the meat compost had a smaller  
227 saturated hydraulic conductivity and larger organic matter content. Hence, the greater  
228 retention at the dry end may be due to the larger specific surface area provided by this  
229 additional organic matter (Khaleel et al, 1981).

230           The addition of green compost to the clay loam (Figure 1b) caused a reduction in  
231 retention at all pressures except 0, 30 and 50 cm ( $p < 0.05$ ). This was associated with a  
232 decrease in  $\theta_{res}$  ( $p < 0.04$ ) but a increase in  $\theta_{sat}$  ( $p < 0.02$ ) and therefore total porosity (Table 1).

233 This indicated a decrease in microporosity and an increase in macroporosity. Meat compost,,  
234 on the other hand, increased retention at 0, 30, and 50 cm pressures ( $p < 0.02$ ), suggesting an  
235 increase in macroporosity. The saturated and unsaturated hydraulic conductivity of the clay  
236 loam was increased by the application of both composts (at all pressures with green compost,  
237  $p < 0.01$ , and at 0 and between 30 and  $10^4$  cm with meat compost,  $p < 0.05$ ). The reduction in  
238 water retention caused by green compost contrasted with other studies, which found compost  
239 to increase retention for a series of clay, loam and clay loam soils (Aggelides and Londra,  
240 2000; Reynolds et al., 2009). Conversely, the effect of meat compost corroborates these  
241 studies and agrees with Khaleel et al. (1981) who suggested the addition of organic matter to  
242 fine textured soils primarily increases retention around field capacity.

243         The addition of compost to the clay cap material in the field (Figure 1d) increased  
244 retention at pressures less than 500 cm for all of the three application rates ( $p < 0.05$ ).  
245 Retention increased with increasing application rate for pressures up to 100 cm, however, this  
246 was only significant between the rate of 250 t/ha and the two larger rates ( $p < 0.05$ ). The  
247 saturated hydraulic conductivity also increased with compost application rate ( $p < 0.03$ ). This  
248 increase in conductivity and retention at the wet end of the release curve associated with an  
249 increase in  $\theta_{\text{sat}}$  (Table 1) is explained by an increase in macroporosity and in dominant pore  
250 size (Figure 2d). However, the small difference between 500 and 750 t/ha is consistent with  
251 the results of Aggelides and Londra (2000), who found application rate had no significant  
252 effect on clay.

253

#### 254 *Dominant pore size and physical quality parameters*

255 The diesel-spiked sandy loam had a larger dominant pore size (Figure 2c), represented by a  
256 lower  $h_i$  (Table 2), compared to the uncontaminated sandy loam ( $p < 0.01$ ). This supports the  
257 results of Hyun et al. (2008) who found a larger dominant pore size in a diesel-spiked soil

258 compared to its bioremediated counterpart. However, this shift in pore size may not be as  
259 pronounced as suggested in Figure 2c because it may be partly reflective of changes in  
260 interfacial properties caused by diesel rather than changes in pore size distribution alone. This  
261 artefact results in a large S index despite other parameters being indicative of poor quality  
262 (Table 2). Diesel contamination results in a larger DP ( $p < 0.01$ ), and smaller PAWC ( $p < 0.05$ ),  
263 and RFC ( $p < 0.05$ ).

264 The addition of both composts to the diesel-spiked soil did not significantly alter the  
265 dominant pore size, S, PAWC, DP or RFC (Table 2). DP, RFC and PAWC were less than  
266 optimum, suggesting little improvement in water availability despite the large compost  
267 application rate. The addition of meat compost to the sandy loam ( $p < 0.04$ ) and green compost  
268 to the clay loam ( $p < 0.01$ ) increased the dominant pore size (Figures 2a and 2b, Table 2). The  
269 S index increased in the clay loam ( $p < 0.01$ ) but not in the sandy loam. For both soils, DP  
270 increased significantly while PAWC and RFC decreased. However, whilst these parameters  
271 were within optimum ranges for the sandy loam, clay loam showed poor physical quality and  
272 an aeration deficit.

273 The dominant pore size of the field clay subsoil increased significantly following  
274 compost addition (Figure 2d, Table 2) but the difference between application rates was not  
275 significant. The S index was above optimum for all three rates but greatest for 500 t/ha. DP  
276 remained below optimum whereas PAWC only exceeded the optimum value in the 500 t/ha  
277 treatment. RFC, remained large and outside the optimum range. These results indicate that  
278 the soils suffer from poor aeration and an excess of water but that this water is not always  
279 available for the plant. Hence, the improvement in the hydraulic properties of the  
280 structureless clay subsoil remains limited despite the large compost application rate used.

281

282 *Numerical simulation of water flow in amended soil profiles*

283 A typical field profile description is shown in Figure 3. All profiles showed similar features.  
284 For all application rates, the compost layer, which had a granular texture, formed a distinctive  
285 boundary with the underlying dark grey clay that was massive, structureless and contained  
286 some brick like debris. The compost had been incorporated to a depth of approximately 10  
287 cm in all application rates and plant roots were unable to penetrate the clay subsoil.

288 The capacity of the profiles to retain water was examined by calculating the overall  
289 water storage for both the compost layer and the clay subsoil. The water storage is analysed  
290 in relation to the plant available water capacity, where storage corresponding to moisture  
291 contents lower than 50% available water or higher than field capacity are considered likely to  
292 induce plant stress. For 250 t/ha, the compost layer had a moisture content of less than 50%  
293 available water for 322 days out of 731 days, suggesting this profile was very dry (Figure 4a).  
294 The longest period in which the moisture content was continuously below 50% available  
295 water was 32 days (Table 3). In contrast, for 750 t/ha, the compost layer had a moisture  
296 content above field capacity for 293 days, with periods of up to 32 days continuously above  
297 field capacity (Figure 4c). For 500 t/ha, the compost layer had only 126 days in which the  
298 moisture content was above field capacity and 219 days in which it was less than 50%  
299 available water (Figure 4b). The clay subsoil had a moisture content within optimum ranges  
300 for most of the simulation period (Figure 4d). However, since roots were limited to the  
301 compost layer, its moisture content will have more bearing on plant growth than that of the  
302 clay subsoil. The excessive moisture content in the soil amended at 750 t/ha was reflected in  
303 the yields of the field crops (Lord and Green, 2011) with only the reed canary grass, which is  
304 a wetland species, producing a commercial yield.

305 To illustrate the influence of the clay subsoil on the hydraulic functioning of the  
306 profiles, the water balance was examined in detail for Day 251. This day saw the largest  
307 amount of rainfall (53.2mm) recorded, which resulted in saturation of the compost layer for

308 all three rates. However, the flow rate became restricted to the saturated hydraulic  
309 conductivity of the clay subsoil (40 mm/d) and positive water pressures of up to 9 cm,  
310 building up at the interface between the compost layers and the clay, indicated that the clay  
311 was acting as a permeability barrier. Over the 2-year period, precipitation rates exceeding the  
312 hydraulic conductivity of the clay resulted in runoff when the profiles became saturated. The  
313 lower volume of runoff generated by the 750 t/ha treatment (Table 3) is explained by the  
314 higher porosity and higher retention capacity of the compost layer, which result in higher  
315 mean water storage, but also its greater hydraulic conductivity which result in a larger  
316 cumulative drainage volume (Table 3).

317         Alternative profile designs were considered to examine how incorporation depth or  
318 the type of subsoil would influence the moisture regime. Simulation of the clay cap amended  
319 with 750 t/ha of compost incorporated to a depth of 30cm instead of 10 cm ( $0.25\text{t/m}^3$  as  
320 opposed to  $0.75\text{t/m}^3$ ), indicated a large reduction, from 293 to 34, in the number of days in  
321 which the compost water storage was above field capacity but an increase, from 0 to 195, in  
322 the number of days in which it was below 50% available water (Figure 5). As such deeper  
323 incorporation seems to increase water availability in the compost layer. This will also  
324 increase the volume of soil available for root growth and therefore access to this available  
325 water. Simulations of water flow in a more permeable sandy loam amended with 750 t/ha of  
326 compost with 30 cm incorporation resulted in a dryer profile (Figure 5). Compared to the  
327 amended clay cap profile, the compost layer in the sandy loam profile had a lower number of  
328 days in which moisture content was above field capacity and a larger number of days in  
329 which both the amended layer and the subsoil had a moisture content below 50% available  
330 water (Figure 5) indicating that the soil profile may be too dry for successful plant growth.

331

332

### 333 **Conclusions**

334 The improvement in water retention and physical quality brought about by large applications  
335 of compost varied with soil type and initial soil quality but were also affected by compost  
336 type and diesel contamination. Compost addition to a sandy loam had little influence on  
337 water retention, pore size distribution and soil physical quality indicators. Diesel  
338 contamination in the same sandy loam reduced retention. Compost did not fully restore  
339 retention and the physical quality parameters showed little improvement in water availability.  
340 Despite an increase in macroporosity and hydraulic conductivity, the compost amended clay  
341 loam had poor physical quality and aeration. Undisturbed field samples from the clay cap  
342 amended with 250, 500 or 750 t/ha had water retention above field capacity and hydraulic  
343 conductivity and physical quality that increased with increasing compost application rate.  
344 Differences between the 500 and 750 t/ha rates were small. Thus there appears to be little  
345 further benefit from applying such large rates of compost. This was also corroborated by the  
346 numerical simulations which indicated shallow incorporation of large amounts of compost  
347 resulted in distinct layering of the soil profile and long periods during which the profile had  
348 inadequate moisture for satisfactory plant growth. Soil amended with 500 t/ha had the most  
349 favourable water regime with a greater number of days in which aeration and water  
350 availability were optimum. Deeper incorporation improved the moisture status of the soil  
351 profile. Conversely, simulations with a more permeable subsoil showed that the depth to  
352 which the profile dried below optimum moisture contents increased, suggesting that deep  
353 incorporation into coarser soils may not always be appropriate.

354

355

356

357

358 **Acknowledgements**

359 This research was supported by Cranfield University and the Waste and Resources Action

360 Programme (WRAP). The field site was established using funding from WRAP and the Life

361 III Environment Programme.

362

363



364 **References**

- 365 Aggelides, S.M. & Londra, P.A. 2000. Effects of compost produced from town wastes and  
366 sewage sludge on the physical properties of a loamy and a clay soil. *Bioresource Technology*,  
367 **71**, 253-9.
- 368 Allen, R.G. 1998. Crop Evapotranspiration Guidelines For Computing Crop Water  
369 Requirements: Guidelines for Computing Crop Water Requirements, *Fao Irrigation and*  
370 *Drainage Paper 56*
- 371 Antizar-Ladislao, B., Lopez-Real, J. & Beck, A.J. 2005. Laboratory studies of the  
372 remediation of polycyclic aromatic hydrocarbon contaminated soil by in-vessel composting.  
373 *Waste Management*, **25**, 281-289.
- 374 Bachmann, J., Ellies, A. & Hartge, K.H. 2000. Development and application of a new sessile  
375 drop contact angle method to assess soil water repellency. *Journal of Hydrology*, **231-232**,  
376 66-75.
- 377 British atmospheric data centre (BADC). 2010. Metoffice MIDAS land surface observation  
378 data. <http://badc.nerc.ac.uk>
- 379 Charles, M.B., Ryan, R., Ryan, N. & Oloruntoba, R. 2007. Public policy and biofuels: The  
380 way forward?. *Energy Policy*, **35**, 5737-5746.
- 381 Dexter, A.R. 2004. Soil physical quality: Part I. Theory, effects of soil texture, density, and  
382 organic matter, and effects on root growth. *Geoderma* , **120**, 201-214.
- 383 Dexter, A.R. & Czyz, E.A. 2007. Applications of s-theory in the study of soil physical  
384 degradation and its consequences. *Land Degradation and Development*, **18**, 369-381.
- 385
- 386 Gandolfi, I., Sicolo, M., Franzetti, A., Fontanarosa, E., Santagostino, A. & Bestetti, G. 2010.  
387 Influence of compost amendment on microbial community and ecotoxicity of hydrocarbon-  
388 contaminated soils. *Bioresource technology* , **101**, 568-575.

389 Hyun, S., Ahn, M., Zimmerman, A.R., Kim, M. & Kim, J. 2008. Implication of hydraulic  
390 properties of bioremediated diesel-contaminated soil. *Chemosphere* , **71**, 1646-1653.

391 Kechavarzi, C., Soga, K., Illangasekare, T. 2005. Two-dimensional laboratory simulation of  
392 LNAPL infiltration and redistribution in the vadose zone. *Journal of Contaminant hydrology*,  
393 **76**, 211-233.

394 Kechavarzi, C., Dawson, Q., Leeds-Harrison, P.B. 2010. Physical properties of low-lying  
395 agricultural peat soils in England. *Geoderma*, **154**, 196-202.

396 Khaleel, R., Reddy, K.R. & Overcash, M.R. 1981. Changes in soil physical properties due to  
397 organic waste applications: *A review. J Environ Qual* , **10**, 133-144.

398 Lord, R. and Green, R., (2011). Performance and characteristics of perennial rhizomatous  
399 grasses grown on non-agricultural land – a sustainable fuel source without food displacement.  
400 In Proceedings of the bioten conference on biomass, bioenergy and biofuels 2010 (A.V.  
401 Bridgewater ed.), CPL Press, 78-93.

402 Reynolds, W.D., Drury, C.F., Tan, C.S., Fox, C.A. & Yang, X.M. 2009. Use of indicators  
403 and pore volume-function characteristics to quantify soil physical quality. *Geoderma* , **152**,  
404 252-263.

405 Riddell-Black, D., 2002. Bioremediation and Economic Renewal of Industrially Degraded  
406 Land by Biomass Fuel Crops (BIORENEW). *European Commission Environment Research*  
407 *Programme. Summary Report*. ISBN 1857058836.

408 Said-Pullicino, D., Massaccesi, L., Dixon, L., Bol, R. & Gigliotti, G. 2010. Organic matter  
409 dynamics in a compost-amended anthropogenic landfill capping-soil. *European Journal of*  
410 *Soil Science*, **61**, 35-47.

411 Semple, K.T., Reid, B.J. & Fermor, T.R. 2001. Impact of composting strategies on the  
412 treatment of soils contaminated with organic pollutants. *Environmental Pollution* , **112**, 269-  
413 283.

414 Šimůnek, J., Šejna, M., Saito, H., Sakai M., & van Genuchten, M. T. 2008. The HYDRUS-  
415 1D Software Package for Simulating the One-Dimensional Movement of Water, Heat, and  
416 Multiple Solutes in Variably-Saturated Media. Department of environmental sciences,  
417 university of California, Riverside.

418 Statsoft. 2010. Statistica, 9.

419 van Genuchten, M.T. 1980. A closed form equation for predicting the hydraulic conductivity  
420 of unsaturated soils. *Soil Science Society of America Journal*, **44**, 892-8.

421 van Genuchten, M.T., Leij, F.J. & Yates, S.R. 1991. The RETC Code for Quantifying the  
422 Hydraulic Functions of Unsaturated Soils.

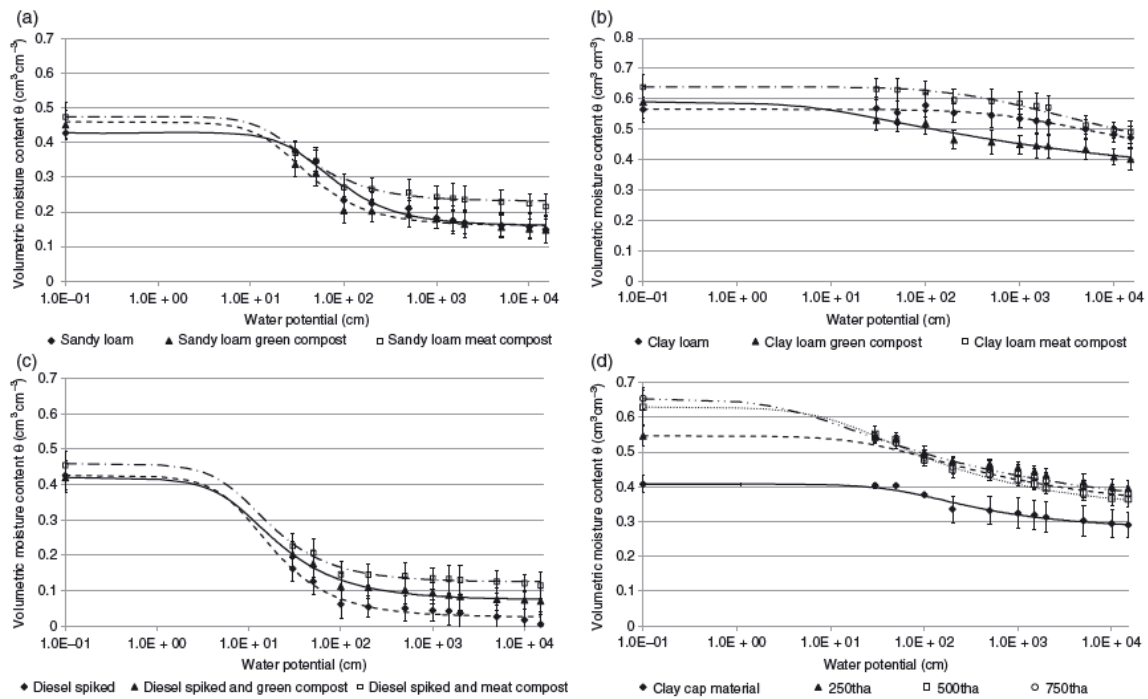
423 Wanas, S.A. & Omran, W.M. 2006. Advantages of applying various compost types to  
424 different layers of sandy soils: Hydro-physical properties. *Journal of Applied sciences*  
425 *research*, **2**, 1298-1303.

426 Whelan A., Kechavarzi C., Sakrabani R., Coulon F., The influence of compost addition on  
427 the hydraulic properties of brownfield soils, proceedings of CONSOIL 2010, 21<sup>st</sup> -24<sup>th</sup>  
428 September 2010, Salzburg, Austria, ISBN: 978-3-00-032099-6.

429

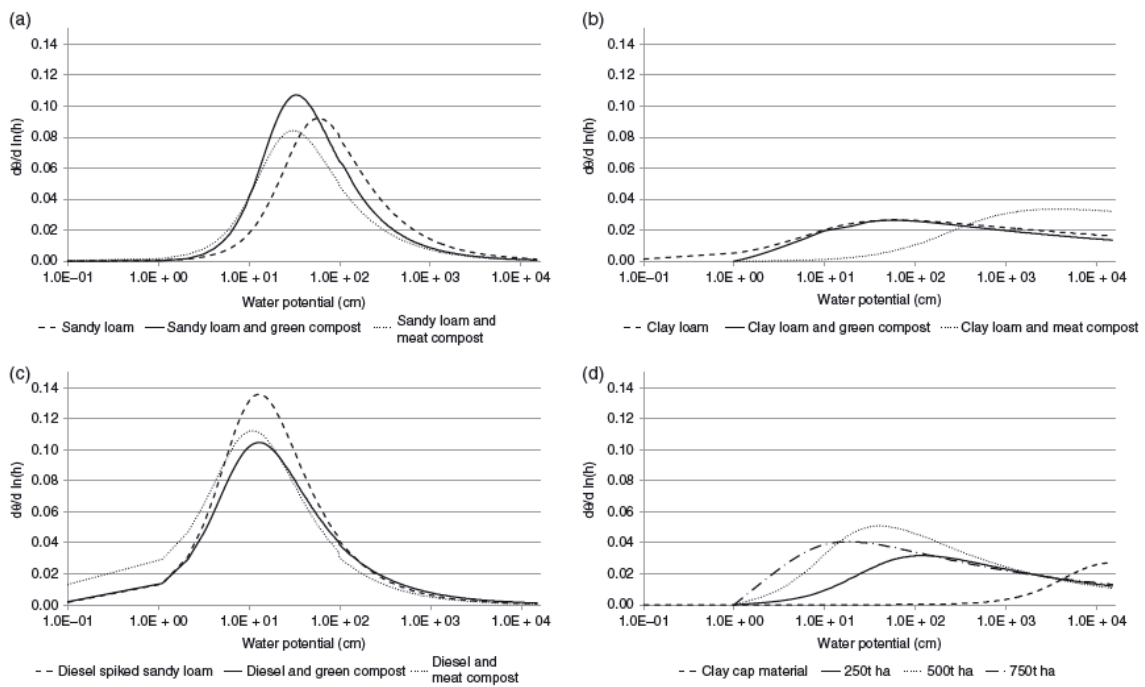
430

431 **Figure Legends**



432

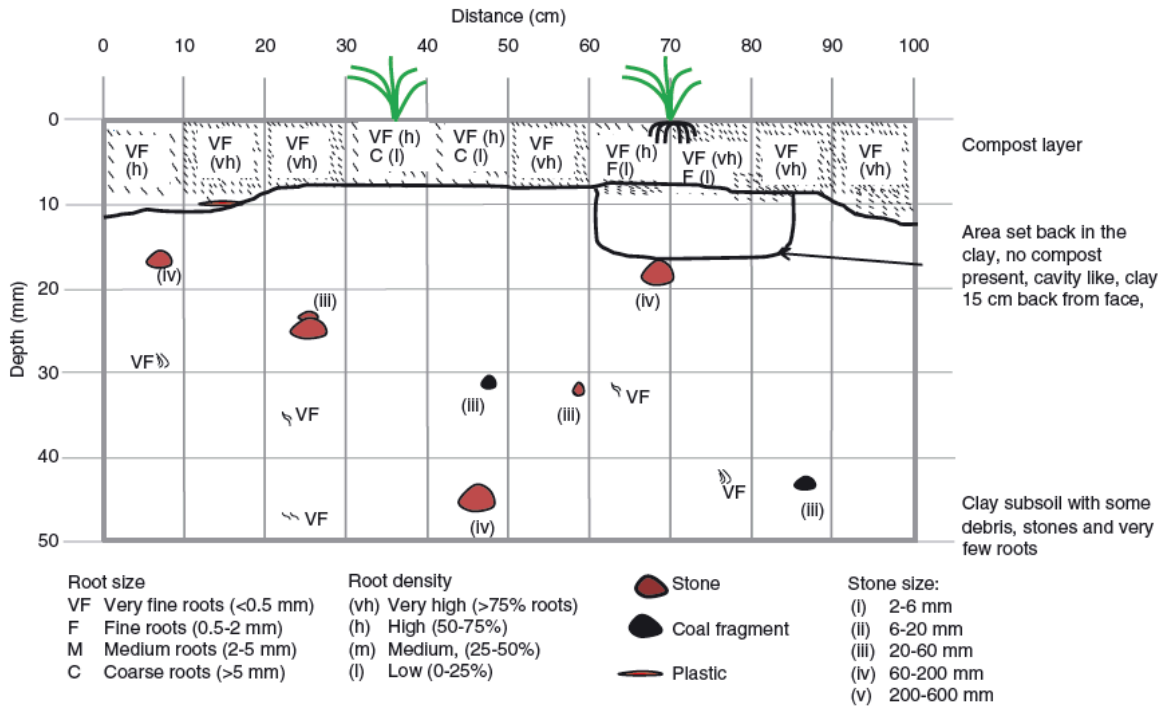
433 Fig. 1. Water release curves of unamended and compost amended soils fitted with the Van  
 434 Genuchten equation: (a) sandy loam; (b) clay loam; (c) diesel spiked sandy loam; (d) field  
 435 clay cap.



436

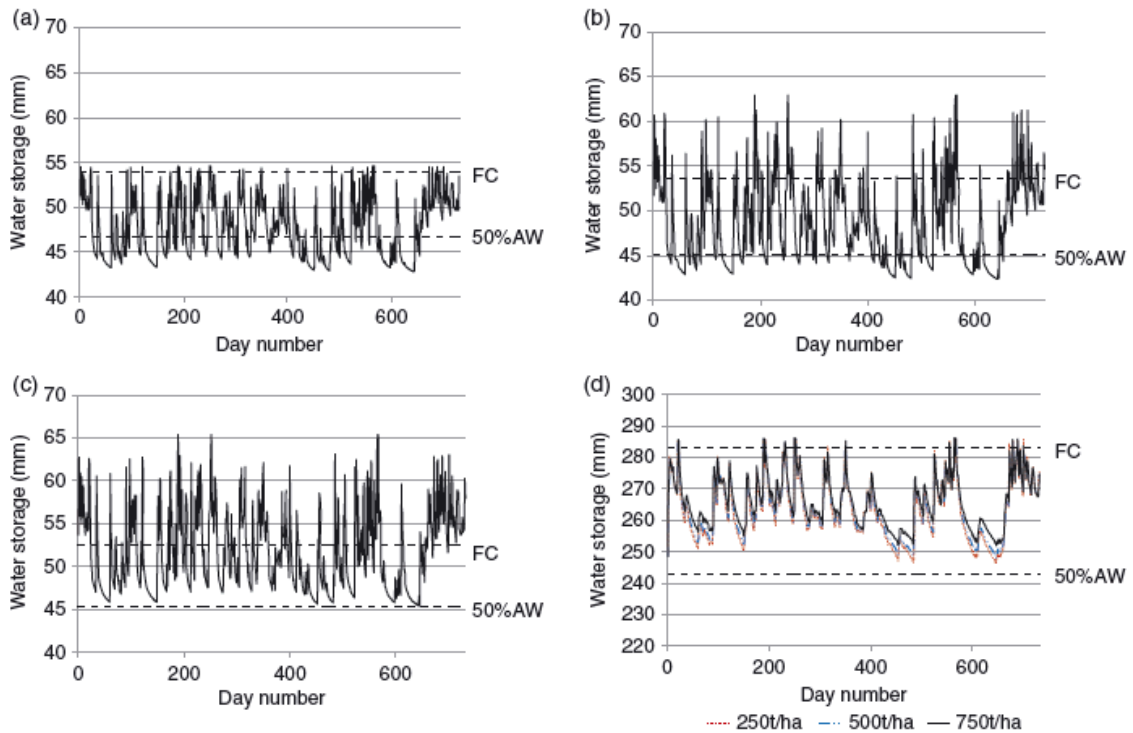
437 Fig. 2. Pore size distribution of unamended and compost amended soils represented by the  
 438 plot of the slope of the release curves against water potential: (a) sandy loam; (b) clay loam;  
 439 (c) diesel spiked sandy loam; (d) field clay cap.

440



441

442 Fig. 3. Typical field profile description: clay cap material amended with 750 t/ha of compost  
 443 to a depth of 10 cm and planted with reed canary grass.

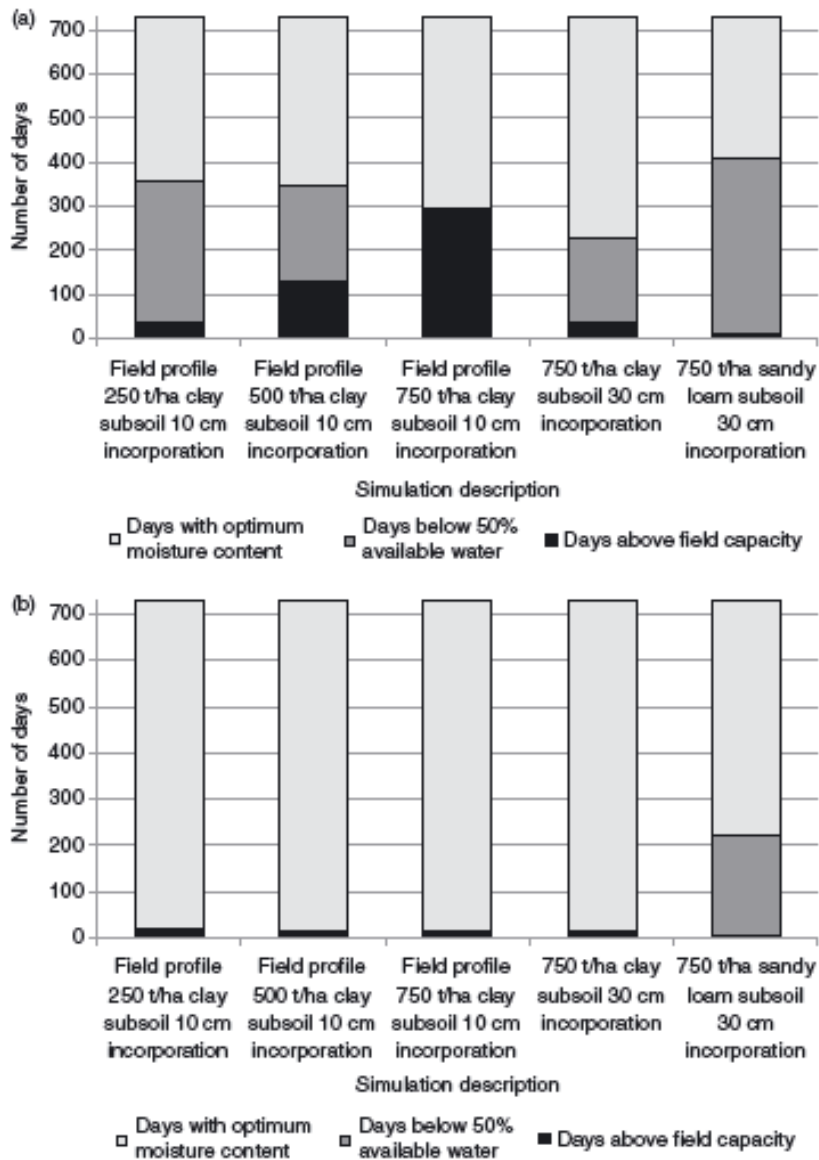


444

445 Fig. 4. Mean water storage in the 10 cm compost layer of the field profiles amended at (a)  
 446 250 t/ha, (b) 500 t/ha and (c) 750t/ha. (d) Mean water storage in the 70 cm clay cap subsoil  
 447 layer of the field profiles amended at 250, 500 and 750 t/ha.

448

449



450

451 Fig. 5. Number of days with mean moisture content within optimum range, below 50%  
 452 available water or above field capacity for (a) the compost layer and (b) the subsoil.

453

454

455 Table 1 van Genuchten parameters for water-release curves and moisture content at  
 456 permanent wilting point (PWP), field capacity (FC) and when 50% of the available water  
 457 (AW) is depleted

Sample	$\theta_{sat}$ (cm <sup>3</sup> /cm <sup>3</sup> )	$\theta_{res}$ (cm <sup>3</sup> /cm <sup>3</sup> )	$n$	$\alpha$ (per m)	$1/\alpha$ (m)	$\theta$ PWP (cm <sup>3</sup> /cm <sup>3</sup> )	$\theta$ FC (cm <sup>3</sup> /cm <sup>3</sup> )	50% AW (cm <sup>3</sup> /cm <sup>3</sup> )
Sandy loam	0.429	0.160	1.852	2.586	0.387	0.151	0.348	0.249
Sandy loam and green compost	0.460	0.161	1.905	4.514	0.222	0.149	0.313	0.231
Sandy loam and meat compost	0.476	0.232	1.859	4.864	0.206	0.217	0.348	0.283
Diesel-spiked sandy loam	0.427	0.026	1.839	11.540	0.087	0.006	0.127	0.066
Diesel-spiked and green compost	0.420	0.074	1.714	12.554	0.08	0.071	0.176	0.123
Diesel-spiked and meat compost	0.460	0.125	1.826	12.502	0.08	0.115	0.208	0.161
Green compost	0.563	0.264	1.748	11.653	0.086	0.256	0.363	0.310
Meat compost	0.550	0.297	1.993	8.935	0.112	0.290	0.367	0.329
Clay loam	0.566	0.223	1.108	0.136	7.353	0.473	0.564	0.518
Clay loam and green compost	0.590	0.310	1.139	12.925	0.077	0.402	0.523	0.462
Clay loam and meat compost	0.640	0.001	1.067	0.369	2.711	0.491	0.634	0.562
Field samples 250 t/ha	0.546	0.326	1.246	3.110	0.322	0.396	0.539	0.467
Field samples 500 t/ha	0.629	0.328	1.308	7.616	0.131	0.366	0.536	0.451
Field samples 750 t/ha	0.654	0.319	1.195	25.858	0.039	0.379	0.526	0.453
Field clay cap material	0.408	0.279	1.421	1.520	0.658	0.291	0.404	0.347

458

459

460 Table 2 Physical quality parameters of all soils with optimum suggested values

Sample	Hydraulic conductivity (m/day)	Drainable porosity (cm <sup>3</sup> /cm <sup>3</sup> )	Plant available water (cm <sup>3</sup> /cm <sup>3</sup> )	Relative field capacity	Pressure at inflection point $h_t$ (cm)	Water content at inflection point $\theta_t$ (cm <sup>3</sup> /cm <sup>3</sup> )	Slope at inflection point S
Sandy loam	0.44 (±0.06)	0.081	0.197	0.811	58	0.21	0.10
Sandy loam and green compost	1.02 (±0.46)	0.147	0.163	0.680	33	0.25	0.08
Sandy loam and meat compost	0.17 (±0.06)	0.127	0.131	0.732	31	0.19	0.09
Diesel-spiked sandy loam	4.77 (±1.86)	0.300	0.121	0.297	13	0.31	0.12
Diesel-spiked and green compost	0.89 (±0.20)	0.244	0.105	0.419	13	0.24	0.12
Diesel-spiked and meat compost	0.40 (±0.11)	0.252	0.093	0.452	12	0.25	0.14
Green compost	22.38 (±6.54)	0.199	0.108	0.646	14	0.21	0.09
Meat compost	13.32 (±4.00)	0.183	0.077	0.667	15	0.22	0.10
Clay loam	0.08 (±0.12)	0.001	0.091	0.997	6050	0.49	0.03
Clay loam and green compost	0.39 (±0.09)	0.085	0.121	0.887	60	0.52	0.04
Clay loam and meat compost	0.15 (±0.05)	0.001	0.143	0.991	3650	0.54	0.04
Field samples 250 t/ha	0.07 (±0.01)	0.009	0.143	0.986	118	0.48	0.05
Field samples 500 t/ha	0.47 (±0.76)	0.035	0.170	0.853	40	0.53	0.12
Field samples 750 t/ha	1.22 (±1.39)	0.069	0.147	0.804	18	0.56	0.09
Field clay cap material	0.04 (±0.01)	0.003	0.113	0.989	155	0.36	0.04
Optimum suggested value (Reynolds <i>et al.</i> , 2009)		≥ 0.14	≥ 0.15	0.6–0.7			>0.035

461

462 Tab 3 Drainage, run-off, mean water storage and duration of longest periods above field  
 463 capacity or below 50% available water in compost layer

	Cumulative drainage from bottom of profile (mm)	Run- off (mm)	Mean water storage (mm)	Longest period above Field capacity in compost layer (days)	Longest period below 50% available water in compost layer (days)
Field profile 250 t/ha – clay subsoil – 10 cm incorporation	1184	24.5	47.8	2	32
Field profile 500 t/ha – clay subsoil – 10 cm incorporation	1190	17.7	48.8	5	29
Field profile 750 t/ha – clay subsoil – 10 cm incorporation	1287	15.8	51.7	33	0
750 t/ha – clay loam subsoil – 30 cm incorporation	1160	23.3	146.7	2	28
750 t/ha – sandy loam – 30 cm incorporation	1210	0	70.2	2	46

464



# Influence of compost amendments on the hydraulic functioning of brownfield soils

Whelan, A.

2013-01-21

Attribution-NonCommercial 4.0 International

---

Whelan A, Kechavarzi C, Coulon F. (2013) Influence of compost amendments on the hydraulic functioning of brownfield soils. *Soil Use and Management*, Volume 29, Issue 2, June 2013, pp. 260-270

<https://doi.org/10.1111/sum.12028>

*Downloaded from CERES Research Repository, Cranfield University*